Priority Report

Cancer Research

STK11/LKB1 Deficiency Promotes Neutrophil Recruitment and Proinflammatory Cytokine Production to Suppress T-cell Activity in the Lung Tumor Microenvironment

Shohei Koyama[1,2], Esra A. Akbay[2,3], Yvonne Y. Li[2,3], Amir R. Aref[2,3], Ferdinandos Skoulidis[4], Grit S. Herter-Sprie[2,3], Kevin A. Buczkowski[3], Yan Liu[2,3], Mark M. Awad[2,3], Warren L. Denning[4], Lixia Diao[5], Jing Wang[5], Edwin R. Parra-Cuentas[6], Ignacio I. Wistuba[6], Margaret Soucheray[7], Tran Thai[3], Hajime Asahina[2,3], Shunsuke Kitajima[3], Abigail Altabef[3], Jillian D. Cavanaugh[3], Kevin Rhee[3], Peng Gao[3], Haikuo Zhang[2,3], Peter E. Fecci[8], Takeshi Shimamura[9], Matthew D. Hellmann[10], John V. Heymach[4], F. Stephen Hodi[2,3], Gordon J. Freeman[1,2], David A. Barbie[2,3], Glenn Dranoff[11], Peter S. Hammerman[2,3], and Kwok-Kin Wong[2,3,12]

Downloaded from http://aacrjournals.org/cancerres/article-pdf/76/5/999/2746958/999.pdf by guest on 24 August 2022

Abstract

STK11/LKB1 is among the most commonly inactivated tumor suppressors in non–small cell lung cancer (NSCLC), especially in tumors harboring *KRAS* mutations. Many oncogenes promote immune escape, undermining the effectiveness of immunotherapies, but it is unclear whether the inactivation of tumor suppressor genes, such as *STK11/LKB1*, exerts similar effects. In this study, we investigated the consequences of *STK11/LKB1* loss on the immune microenvironment in a mouse model of *KRAS*-driven NSCLC. Genetic ablation of *STK11/LKB1* resulted in accumulation of neutrophils with T-cell–suppressive effects, along with a corresponding increase in the expression of T-cell exhaustion markers and tumor-promoting cytokines. The number of tumor-infiltrating lymphocytes was also reduced in *LKB1*-deficient mouse and human tumors. Furthermore, *STK11/LKB1*–inactivating mutations were associated with reduced expression of PD-1 ligand PD-L1 in mouse and patient tumors as well as in tumor-derived cell lines. Consistent with these results, PD-1–targeting antibodies were ineffective against *Lkb1*-deficient tumors. In contrast, treating *Lkb1*-deficient mice with an IL6-neutralizing antibody or a neutrophil-depleting antibody yielded therapeutic benefits associated with reduced neutrophil accumulation and proinflammatory cytokine expression. Our findings illustrate how tumor suppressor mutations can modulate the immune milieu of the tumor microenvironment, and they offer specific implications for addressing *STK11/LKB1*–mutated tumors with PD-1–targeting antibody therapies. *Cancer Res; 76(5); 999–1008. ©2016 AACR.*

Introduction

The discovery of a series of oncogene driver mutations and the concept of oncogene addiction has changed the therapeutic approach for subsets of patients with non–small cell lung cancers (NSCLC; ref. 1). While this targeted approach for tumors with specific kinase alterations has been successful, *KRAS* mutation is the most common genetic alteration driving NSCLCs and remains refractory to targeted treatment strategies. *KRAS*-mutated NSCLCs are genomically more complex than those harboring mutated *EGFR* or *EML4-ALK* and the concurrent loss of key tumor suppressors such as *TP53* or *STK11* is common in *KRAS*-mutated lung adenocarcinomas.

STK11/LKB1 is inactivated in approximately one-third of the *KRAS*-mutated lung adenocarcinomas, a frequency comparable with *TP53* loss in this background, though *STK11* and *TP53* mutations rarely overlap in *KRAS*-mutant lung tumors (2).

[1]Department of Medical Oncology and Cancer Vaccine Center, Dana Farber Cancer Institute, Boston, Massachusetts. [2]Department of Medicine, Brigham and Women's Hospital and Harvard Medical School, Boston, Massachusetts. [3]Department of Medical Oncology, Dana Farber Cancer Institute, Boston, Massachusetts. [4]Department of Thoracic/Head and Neck Medical Oncology, The University of Texas MD Anderson Cancer Center, Houston, Texas. [5]Department of Bioinformatics and Computational Biology, The University of Texas MD Anderson Cancer Center, Houston, Texas. [6]Department of Translational Molecular Pathology, The University of Texas MD Anderson Cancer Center, Houston, Texas. [7]University of California, San Francisco, San Francisco, California. [8]Division of Neurosurgery, Department of Surgery, Duke University Medical Center, Durham, North Carolina. [9]Department of Molecular Pharmacology and Therapeutics, Oncology Research Institute, Loyola University Chicago, Illinois. [10]Department of Medicine, Memorial Sloan Kettering Cancer Center, New York, New York. [11]Novartis Institutes for BioMedical Research, Cambridge, Massachusetts. [12]Belfer Institute for Applied Cancer Science, Dana Farber Cancer Institute, Boston, Massachusetts.

Note: Supplementary data for this article are available at Cancer Research Online (http://cancerres.aacrjournals.org/).

S. Koyama, E.A. Akbay, and Y.Y. Li contributed equally to this article.

Corresponding Authors: Kwok-Kin Wong, Dana-Farber Cancer Institute, 44 Binney St, Boston, MA 02115. Phone: 617-582-6084; Fax: 617-582-7839; E-mail: kwong1@partners.org; Peter Hammerman, Novartis Institutes for BioMedical Research, 250 Massachusetts Avenue, Cambridge, MA, 02139. E-mail: peter_hammerman@dfci.harvard.edu; and Glenn Dranoff, Novartis Institutes for BioMedical Research, 250 Massachusetts Avenue, Cambridge, MA, 02139. E-mail: glenn.dranoff@novartis.com

doi: 10.1158/0008-5472.CAN-15-1439

©2016 American Association for Cancer Research.

Lkb1-deficient *Kras*-mutated (*Kras/Lkb1)* tumors show a more invasive and metastatic phenotype with significantly reduced survival (3), and differential drug sensitivities as compared with *Kras*-mutant *Lkb1*-wild-type tumors and *Kras*-mutated compound *Tp53*-deficient animals (4). A more metastatic phenotype in *KRAS/LKB1* tumors has also been described in clinical studies (5, 6).

Recent clinical trials in NSCLC have demonstrated response to immune checkpoint blockade and nominated predictive markers for the efficacy of specific immunotherapies (7–9). Our previous work suggests that oncogenes impact immune evading mechanisms by directly activating immune checkpoints (10). Immune evasion can also be achieved by the release of proinflammatory cytokines into the tumor microenvironment that play an important role in promoting tumor growth, metastasis, and immune suppression (11, 12). Previous work has shown that *Kras*-mutated tumors display activation of the noncanonical IkappaB kinase TBK1 (13, 14), and the activation of this signaling pathway induces several proinflammatory cytokines, such as IL6 and CXC-chemokine ligands. Myeloid cells, especially tumor-associated macrophages (TAM) and neutrophils (TAN), support tumor cell proliferation and impede host immune surveillance through cytokine production and cell–cell interactions (15).

To elucidate how *Stk11/Lkb1* (hereafter referred to as *Lkb1* in the mouse model) loss affects the inflammatory phenotype in *Kras*-driven lung cancer, we compared immune cell populations and cytokine/chemokine profiles among *Kras* and *Kras/Lkb1* mouse lung cancer models. We found that neutrophil-attracting soluble factors and neutrophil numbers were significantly increased and both T-cell numbers and function were significantly decreased in *Lkb1*-deficient tumors. Moreover, *Lkb1* loss of function negatively impacted PD-L1 expression in lung tumor cells in mouse and human tumors and cell lines. By depleting the neutrophils in *Kras/Lkb1*–mutant mice, T-cell numbers and function were significantly improved affirming the immunosuppressive properties of this cell type. Finally, we functionally validated the therapeutic utility of blocking the cytokine feedback loop with a neutralizing anti-IL6 antibody, which resulted in an increase of T-cell numbers and function. Together, the results suggest that in the *Lkb1*-deficient tumors, immune evasion is achieved through suppressive myeloid cells and aberrant cytokine production and not the PD-1:PD-L1 interaction.

Materials and Methods

Murine cell line and *in vivo* studies

Mouse strains were described previously (3). Mice were dosed with 200 μg of IL6-neutralizing antibody (MP5-20F3, BioXcell), anti Ly-6G/Gr-1 antibody (RB6-8C5, BioXcell), PD-1–blocking antibody (clone 29F.1A12), and isotype controls (BioXcell) three times a week via intraperitoneal injections. MRI quantification was performed as described previously (10). Murine cell lines bearing mutated *Kras* and *p53*-loss (*Kras/p53*:KP) and mutated *Kras* and both *p53* and *Lkb1*-loss (*Kras/p53/Lkb1*:KPL) were established and characterized as described previously (16). Recombinant mouse IL1α was from PeproTech.

Immune cell isolation, analysis, and sorting

Lung cell isolation, mononuclear cell enrichment, and characterization of immune cell populations in murine tissue samples were described previously (10). Total cell count was divided by tumor-bearing lung weight utilized for each assay. Antibodies are listed in Supplementary Methods. Intracellular staining for Ki-67, IFNγ, CTLA-4, FOXP3, and LGALS9 was performed according to the manufacturer's protocol (eBioscience and BD Biosciences). Sorting of tumor cells ($CD45^{-}EpCAM^{+}$) and neutrophils ($CD45^{+}CD11b^{+}Ly\text{-}6G^{+}$) was performed on a BD FACSAria II. Gating methods for immune analysis and sorting are mentioned in Supplementary Methods.

Sample preparation for RNA sequencing

RNA isolation from sorted cells was performed using the PicoPure RNA Isolation Kit (Life Technologies) according to the manufacturer's protocol. Ten to 100 ng of total RNA was used as input for the generation libraries using the Nugen Ovation Kit. Libraries were quality controlled on an Agilent high sensitivity DNA chip and sequencing of pooled libraries was performed on the Illumina HiSeq platform to a minimum depth of 30 million reads.

Mouse RNA sequencing and patient tumor gene expression and proteomic data analysis (CCLE, TCGA, and PROSPECT)

For details, see Supplementary Methods.

Preparation of isogenic human cell lines and IL1-α stimulation

Human lung cancer cell lines were obtained from ATCC and used prior to 6 months of passage in culture and not further authenticated. Short hairpin RNA constructs and stable isogenic cell lines were established as described previously (17). Recombinant human IL1α was from PeproTech (18).

IHC

IHC for TUNEL and Ki-67 was performed as previously described (19). For the PROSPECT samples, 4-μm thick tissue sections were stained using an automated staining system (Leica Bond Max, Leica Microsystems), according to the standard protocols. The38 Aperio Image Analysis Toolbox (Aperio, Leica Microsystems) was used for digital analysis of images obtained from scanned slides. PDL1 clone E1L3N from Cell Signaling Technology, CD3 A0452 from Dako, and CD8 C8/144B from Thermo Scientific were used.

Western blotting

Tumor nodules resected from *Kras* and *Kras/Lkb1* mice were homogenized in RIPA buffer and proteinase inhibitor (Cell Signaling Technology). Western blotting was performed as described previously (18) with anti pSTAT3, STAT3, LKB1, and actin antibodies (Cell Signaling Technology).

Measurement of soluble factor concentrations in bronchoalveolar lavage fluids from mice and culture supernatants from murine and human cell lines

For details, see Supplementary Methods.

Statistical analysis

All numerical data are presented as mean ± SD. Data were analyzed using two-tailed unpaired Student *t* test for comparisons of two groups and one-way ANOVA with Tukey post-test for three groups. *P* values for the survival curves have been calculated using a log-rank test. Mann–Whitney *U* tests were used to assess correlation of PD-L1 and T-cell markers in human tumor samples with LKB1 status. Multivariate testing of The Cancer Genome Atlas (TCGA) data with respect to genotype and clinical factors (sex,

Downloaded from http://aacrjournals.org/cancerres/article-pdf/76/5/999/2746958/999.pdf by guest on 24 August 2022

primary tumor stage, nodal stage, metastasis stage, overall stage, age, and smoking) was performed using one-way ANOVA.

Results

Lkb1-deficient tumor cells stimulate neutrophil recruitment through the production of cytokines and chemokines

We previously showed that oncogene activation contributes to escape from immune surveillance by modulating the tumor microenvironment (10). However, the loss of tumor suppressors has not been previously investigated in this context. To elucidate how *Lkb1* deficiency impacts the immune microenvironment in lung tumors, we compared the immune cell populations and cytokine profiles of *Kras* and *Kras/Lkb1* mouse models with similar degrees of tumor burden (Supplementary Fig. S1A). We found that *Lkb1*-deficient tumors showed a greater variation in the number of total hematopoietic ($CD45^+$) cells (Supplementary Fig. S1B) and an increase in the total $CD11b^+$ myeloid cell population among three major clusters ($CD11c^-CD11b^-$, $CD11c^+CD11b^-$, $CD11b^+$) in the lung (Fig. 1A). Detailed analysis of these myeloid cell populations showed that total numbers of TAN ($CD11b^+Ly\text{-}6G^+$) are significantly elevated and tumor-associated alveolar macrophages (TAM: $CD11c^+CD11b^-CD103^-$) are significantly decreased in *Kras/Lkb1* tumors compared with *Kras* tumors (Fig. 1A). Minor myeloid cell populations including eosinophils, Ly-$6C^{hi}$ inflammatory monocytes, and $CD103^+$ dendritic cells did not show significant differences (Supplementary Fig. S1C). Interestingly, the increase of neutrophils was also observed in the spleen and peripheral blood of *Kras/Lkb1* mice (Fig. 1B).

To identify the cytokines and chemokines driving the immune phenotype of *Lkb1*-deficient tumors, we sorted $CD45^-EpCAM^+$ cells from *Kras* and *Kras/Lkb1* lung tumors using FACS and performed mRNA sequencing. We discovered higher expression of a number of chemokines in the *Kras/Lkb1* tumor cells: *Ppbp* [proplatelet basic protein: chemokine (C-X-C motif) ligand 7 (*Cxcl7*)], *Cxcl3*, and *Cxcl5*, all of which act through chemokine receptor CXCR2 on neutrophils (Supplementary Methods), and cytokines: *Csf3* [colony stimulating factor 3: granulocyte colony stimulating factor (*G-Csf*)] and two of the IL1 family of proinflammatory cytokines, *Il33* and *Il1α* (Fig. 1C). On the contrary, we identified a decrease in the expression of chemokine (C-C motif) ligand 5 (*Ccl5*) and *Cxcl12* in *Kras/Lkb1* tumor cells as compared with *Kras*. Both of these chemokines play an important role in recruiting lymphocytes and dendritic cells (20, 21) and these cell types are underrepresented in *Kras/Lkb1* tumors (Supplementary Fig. S1C and S1D).

In addition to tumor cells, we sorted TAN from *Kras/Lkb1* tumors and compared gene expression profiles with TAN from the uninduced normal lung from mice with the same genetic background. Analysis of mRNA sequencing revealed that TAN from the *Kras/Lkb1* tumors produced elevated T-cell–suppressive factors (22) including *Il10*, *Lgals9*, Arginase 1 (*Arg1*), and Milk fat globulin EGF factor 8 protein (*Mfge8*) and the tumor-promoting cytokine, *Il6*, as compared with neutrophils from normal lung (Supplementary Fig. 2A).

To confirm these findings at the protein level, we analyzed CXCL7, G-CSF, and IL1α in culture supernatants from cell lines derived from mouse tumors (16). There was a significant increase in CXCL7 and G-CSF in *Kras*-mutated *Tp53*-deficient *Lkb1*-deficient cell lines (KPL) compared with *Kras*-mutated *Tp53*-deficient *Lkb1*-wild type cell lines (KP; Fig. 1D) but IL1α was under the detection limit in all cell lines (data not shown). In addition to the cytokines identified as differentially expressed in mRNA sequencing, we analyzed IL6 and IL17, two well-characterized cytokines that contribute to neutrophil accumulation and production (23, 24), and found that IL6 was significantly increased in KPL compared with KP (Fig. 1D), but IL17 was not detected (data not shown). Of the cytokines in bronchoalveolar lavage fluids (BALF), CXL7 showed significant difference in *Kras/Lkb1* versus control and G-CSF, MFG-E8, and IL10 in *Kras/Lkb1* versus control and Kras (Fig. 1E and Supplementary Fig. S2B). While *Il6* upregulation was not apparent at the mRNA level in $EpCAM^+$ *Kras/Lkb1* tumors cells (data not shown), we detected the cytokine in BALFs from *Kras/Lkb1* lungs and in cultured sorted $CD45^-EpCAM^+$ cells and TAN from *Kras/Lkb1* tumors (Supplementary Fig. S2C). Considering the higher number of neutrophils in *Kras/Lkb1* tumors as compared with *Kras* tumors, TANs likely play an important role in aberrant production of this cytokine in addition to tumor cells. Given that IL6 mediates its downstream effects through STAT3 (25), we measured the levels of phosphorylated STAT3. We found that *Kras/Lkb1* tumor tissue had higher levels of phospho-STAT3 (pSTAT3) than the *Kras* tumors (Fig. 1F). These findings suggest that *Lkb1* inactivation is associated with neutrophil accumulation to the immune microenvironment and overproduction of tumor-promoting cytokines.

In concordance with RNA sequencing data, IL1α showed a significant increase in BALFs in *Kras/Lkb1* versus that from control (Fig. 1G). Mouse BALFs, similar to the supernatants from cultured cells, did not have detectable IL17 (data not shown). To assess whether IL1α might promote feed forward cytokine signaling in *Lkb1*-deficient tumors, we stimulated a *Kras*-mutated, *p53*-loss, *Lkb1*-loss mouse lung cancer cell line (KPL cell line) with IL1α and analyzed cytokine secretion. Among the cytokines, we detected an increase in IL6, CXCL7, and G-CSF production in a dose-dependent manner (Fig. 1H and Supplementary Fig. S3A). These results are consistent with *Lkb1*-loss increasing IL1α production, which then promotes the activation of IL6–STAT3 signaling.

Lkb1 loss negatively impacts the number and function of tumor infiltrating T cells and PD-L1 expression on tumor cells

Clinical studies have demonstrated that the density of tumor-infiltrating lymphocytes is associated with a favorable prognosis and response of immunotherapy in cancer (7–9). We found that total counts of both CD4 and CD8 T cells were significantly decreased in *Kras/Lkb1* mouse tumors (Fig. 2A) as compared with *Kras* tumors. Infiltrating T cells showed a significantly higher expression of T-cell–inhibitory markers: Programmed cell death protein 1 (PD-1), T-cell immunoglobulin mucin-3 (TIM-3), Lymphocyte-activation gene 3 (LAG-3), and CTL-associated protein 4 (CTLA-4; Fig. 2B). We also confirmed expression of the ligand for TIM-3, LGALS9, in both tumor cells and TAN from *Kras/Lkb1* tumors by flow cytometry (Supplementary Fig. S2D). The ratio of regulatory T cells ($FOXP3^+$) to total CD4 T cells was also significantly increased in *Kras/Lkb1* tumor as compared with *Kras* tumors (Fig. 2B). We evaluated T-cell function in *Kras/Lkb1* and *Kras* tumors with similar levels of disease (Supplementary Fig. S3B) and found significantly less IFNγ and Ki-67 expression in total CD4 and CD8 T cells from the *Kras/Lkb1* tumors than those from *Kras* tumors (Fig. 2C). Thus, *Lkb1* inactivation is associated with reduced T-cell number and increased markers of T-cell exhaustion.

Downloaded from http://aacrjournals.org/cancerres/article-pdf/76/5/999/2746958/999.pdf by guest on 24 August 2022

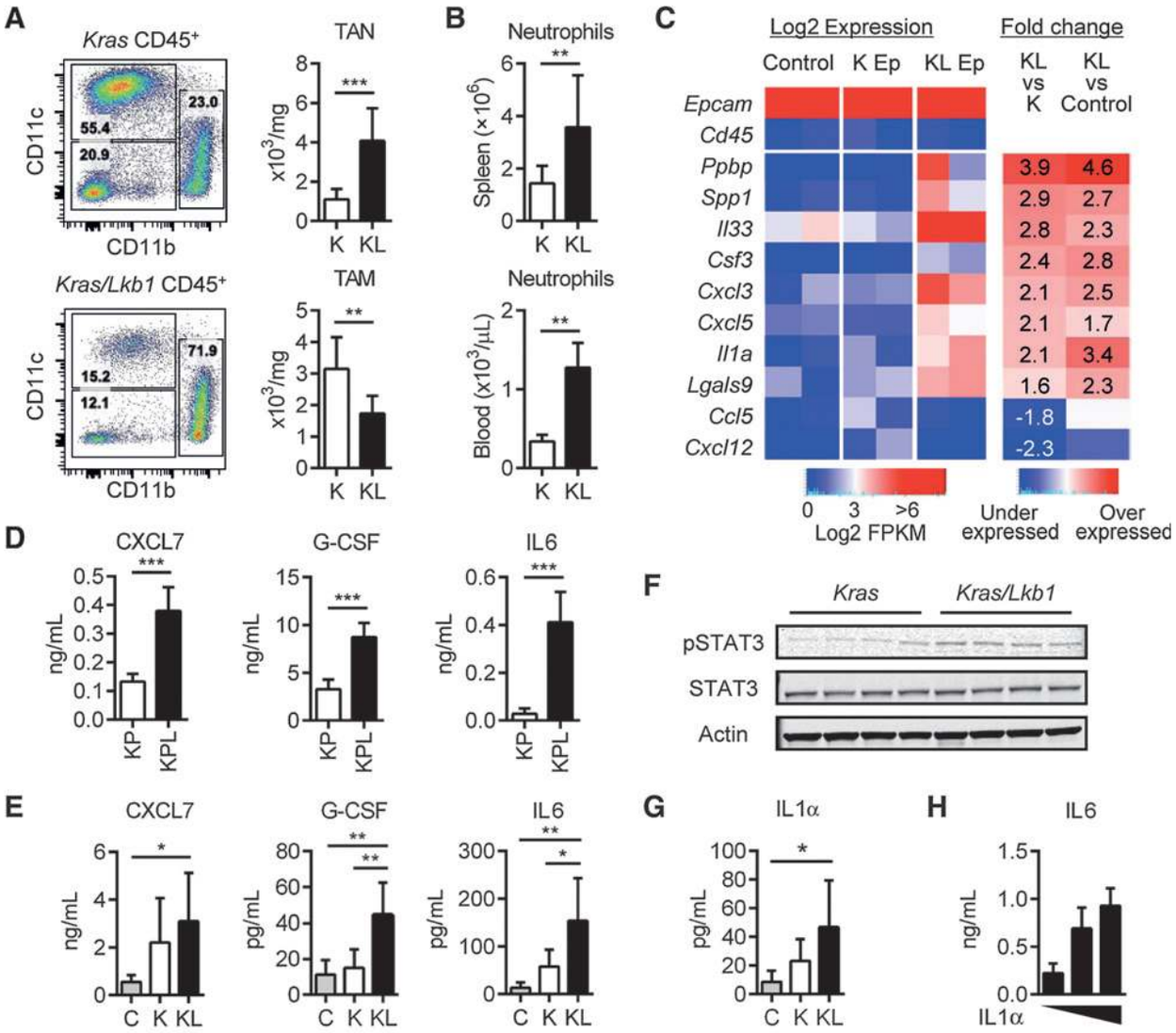

Figure 1.

Tumor-suppressor *Lkb1* inactivation promotes neutrophil accumulation via proinflammatory cytokines and chemokines. A, immune cell populations in the lung tumors from *Kras* (K) and *Kras/Lkb1* (KL) mouse models. Representative flow cytometry data (live/single/total CD45$^+$ cells) from each mouse model (left). Total counts of TAN: CD11b$^+$Ly-6G$^+$ cells and TAMs: CD11c$^+$CD11b$^-$CD103$^-$ from *Kras* (K; $n = 8$) and *Kras/Lkb1* (KL; $n = 8$) mice. **, $P < 0.01$; ***, $P < 0.001$. B, neutrophil counts in the spleen and peripheral blood from *Kras* ($n = 8$) or *Kras/Lkb1* ($n = 8$) mice (right). **, $P < 0.01$. C, expression of immune-modulating factors from RNA sequencing of the sorted tumor cells (CD45$^-$EpCAM$^+$) in *Kras* (K Ep) or *Kras/Lkb1* (KL Ep) mice and uninduced normal lung CD45$^-$EpCAM$^+$ cells (control). Each column consists of a combination of samples derived from 3 to 4 mice. Log-transformed FPKM values are shown, colored blue/red for low/high expression, respectively. *Epcam* and *Cd45* expression are shown as positive and negative controls. Differential expression is shown as fold-change values, colored blue/red for under/overexpression compared with controls. D and E, chemokine and cytokine levels in the culture supernatants after 48-hour incubation from *Kras/p53* (KP; $n = 3$) versus *Kras/p53/Lkb1* (KPL; $n = 3$) cell lines generated from mouse lung tumors; ***, $P < 0.001$. Data indicate three replicate wells and are representative of three independent experiments (D) and BALF from littermate controls ($n = 5$), *Kras* mice ($n = 8$) or *Kras/Lkb1* mice ($n = 8$; E). *, $P < 0.05$; **, $P < 0.01$. F, Western blot analysis for pSTAT3, STAT3 levels in *Kras* versus *Kras/Lkb1* tumors. Each column represents tumor from a different mouse and actin represents loading control. G, IL1α level in the BALF from C ($n = 5$), *Kras* ($n = 8$), or *Kras/Lkb1* ($n = 8$) mice. *, $P < 0.05$. H, IL6 levels in culture supernatants measured 24 hours after IL1α stimulation (0, 5, and 20 ng/mL) of KP ($n = 3$) versus KPL ($n = 3$) cell lines. Data indicate three replicate wells and are representative of three independent experiments.

To understand the role of neutrophils in this model, we used a neutrophil-depleting (anti-Ly-6G/Gr-1:RB6-8C5) antibody in mice with established tumors (Supplementary Fig. S4A and S4B). *Kras/Lkb1* mice treated with anti Ly-6G/Gr-1 antibody for 1 or 2 weeks showed a significant reduction of TAN and of IL6 and G-CSF in BALFs (Supplementary Fig. S4C and S4D), resulting in a significant increase in total CD8 T-cell numbers, proliferation (Ki-67$^+$), and T-cell function represented by IFNγ production (Supplementary Fig. S4E).

PD-L1 expression on tumor cells is a biomarker associated with a response to PD-1 blockade treatment (7, 10). *Lkb1*-deficient tumor cells expressed significantly lower levels of PD-L1 in

Downloaded from http://aacrjournals.org/cancerres/article-pdf/76/5/999/2746958/999.pdf by guest on 24 August 2022

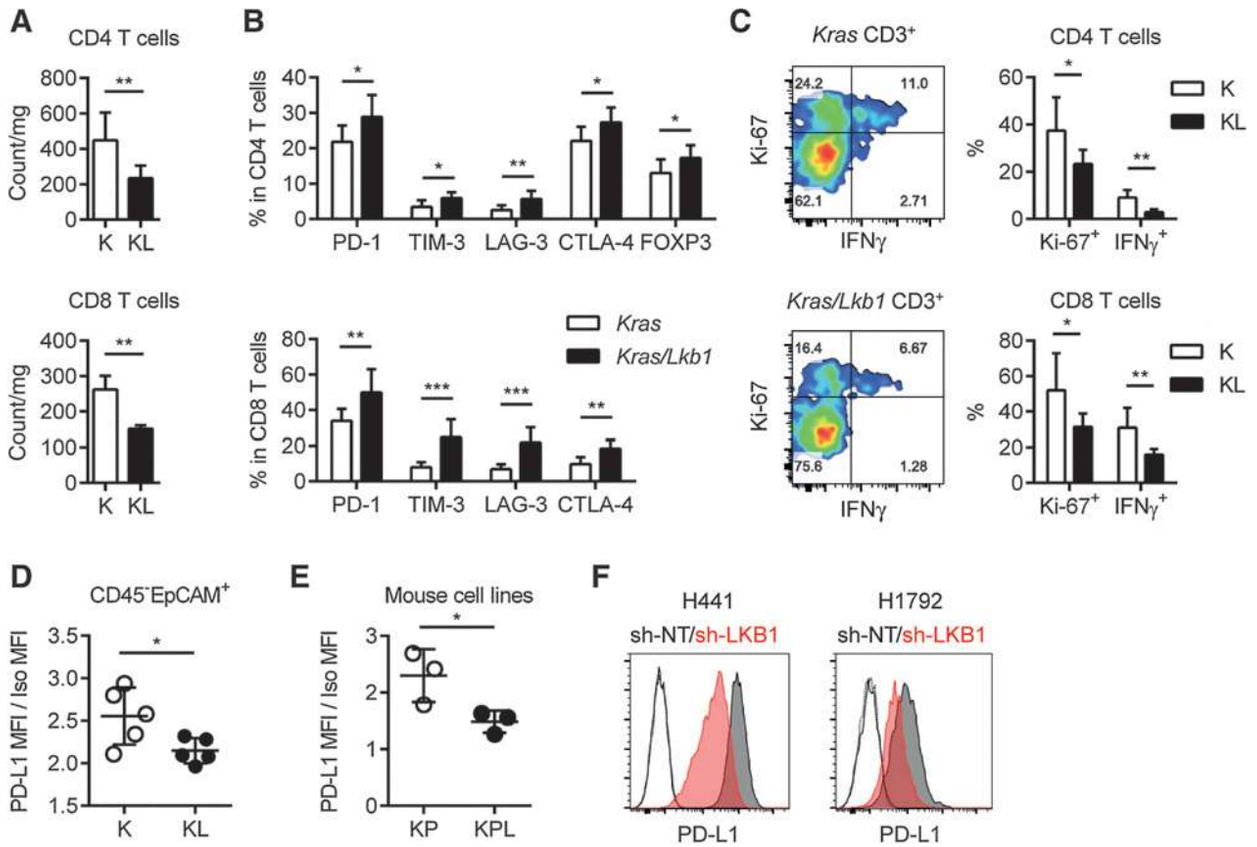

Figure 2.

Lkb1 inactivation leads to a T-cell–suppressive tumor microenvironment with low PD-L1 expression in tumor cells. A, total counts of CD4 T cells (top) and CD8 T cells (bottom). **, $P < 0.01$. B, expression of checkpoint receptors in CD4 T cells (top) and CD8 T cells (bottom) in *Kras* (K) or *Kras/Lkb1* (KL) tumors. *, $P < 0.05$; **, $P < 0.01$; ***, $P < 0.001$. C, IFNγ expression and proliferation marker (Ki-67) positivity for CD4 or CD8 T cells in *Kras* or *Kras/Lkb1* tumors. Representative flow cytometry data (total $CD3^+$ T cells) from each mouse model (left). Percentage of Ki-67^+ and $IFN\gamma^+$ in CD4 or CD8 T cells from *Kras* ($n = 6$) or *Kras/Lkb1* ($n = 6$) mice. *, $P < 0.05$; **, $P < 0.01$. D, PD-L1 expression in gated $CD45^-EpCAM^+$ cells in *Kras* ($n = 5$) or *Kras/Lkb1* ($n = 5$) tumors evaluated by flow cytometry. *, $P = 0.0384$. E, PD-L1 expression in KP ($n = 3$) versus KPL ($n = 3$) cell lines evaluated by flow cytometry. *, $P = 0.0495$. Data are representative of three independent experiments. F, PD-L1 expression in H441 or H1792 cells stably transfected with sh-nontarget (NT) or sh-LKB1. Data are representative of three independent experiments.

$CD45^-EpCAM^+$ cells as compared with *Kras* tumor cells (Fig. 2D). PD-L1 expression is influenced by a variety of factors that include non–cell-autonomous factors such as release of IFNγ from T cells (26) in the tumor microenvironment *in vivo*. To dissect the intrinsic role of *Lkb1* inactivation on PD-L1 expression specifically in tumor cells, we analyzed PD-L1 expression in cultured cell lines derived from mouse tumors of the KP and KPL genotypes. PD-L1 levels were significantly lower in KPL as compared with KP (Fig. 2E). To confirm that our findings in mouse models and cell lines were applicable to humans, we studied human lung cancer cell lines with endogenous *KRAS* mutation and wild-type or inactivated *LKB1*. We either performed knockdown of *LKB1* using shRNA or reconstituted LKB1 with wild-type (WT) or kinase dead (KD) LKB1 to develop isogenic cell lines (wild -type cells: H441, H1792, and *LKB1*-mutant cell: A549; Supplementary Fig. S5A). PD-L1 expression was lower in both of the LKB1 WT lines when expressing sh-LKB1 (Fig. 2F). Expression of *LKB1* (WT and KD) in the *LKB1*-deficient A549 cell line resulted in a modest increase in PD-L1 levels (Supplementary Fig. S5B). These data suggest *LKB1* inactivation decreased PD-L1 levels independent of IFNγ.

Functional loss of *LKB1* in human cell lines is phenotypically similar to mouse *Kras*/*Lkb1* tumors

We next assessed the cytokine and chemokine profiles in human isogenic cell lines to determine whether similar patterns would be observed. We analyzed culture supernatants from these cell lines and found that IL6 and G-CSF were significantly increased in *LKB1*-inactivated cells as compared with *LKB1*-intact cells (Fig. 3A and Supplementary Fig. S5C). There was also a significant increase of CXCL7 that was only detected in A549 cells (Supplementary Fig. S5C). IL1α stimulation of these cell lines led to an increase in IL6, G-CSF, and CXCL7 in a dose-dependent manner (Fig. 3B and Supplementary Fig. S5D), which was consistent with the *Lkb1*-deficient mouse cell line data (Fig. 1D). We also found that IL6 induction by IL1α stimulation was more pronounced in *LKB1*-deficient cell lines as compared with *LKB1*-intact cell lines (Supplementary Fig. S5E) except for H1792, which showed modest stimulation. This line has high baseline IL1α production (Fig. 3A) and the shRNA only partially knocked down *LKB1* (Supplementary Fig. S5A), which makes this result difficult to interpret.

Downloaded from http://aacrjournals.org/cancerres/article-pdf/76/5/999/2746958/999.pdf by guest on 24 August 2022

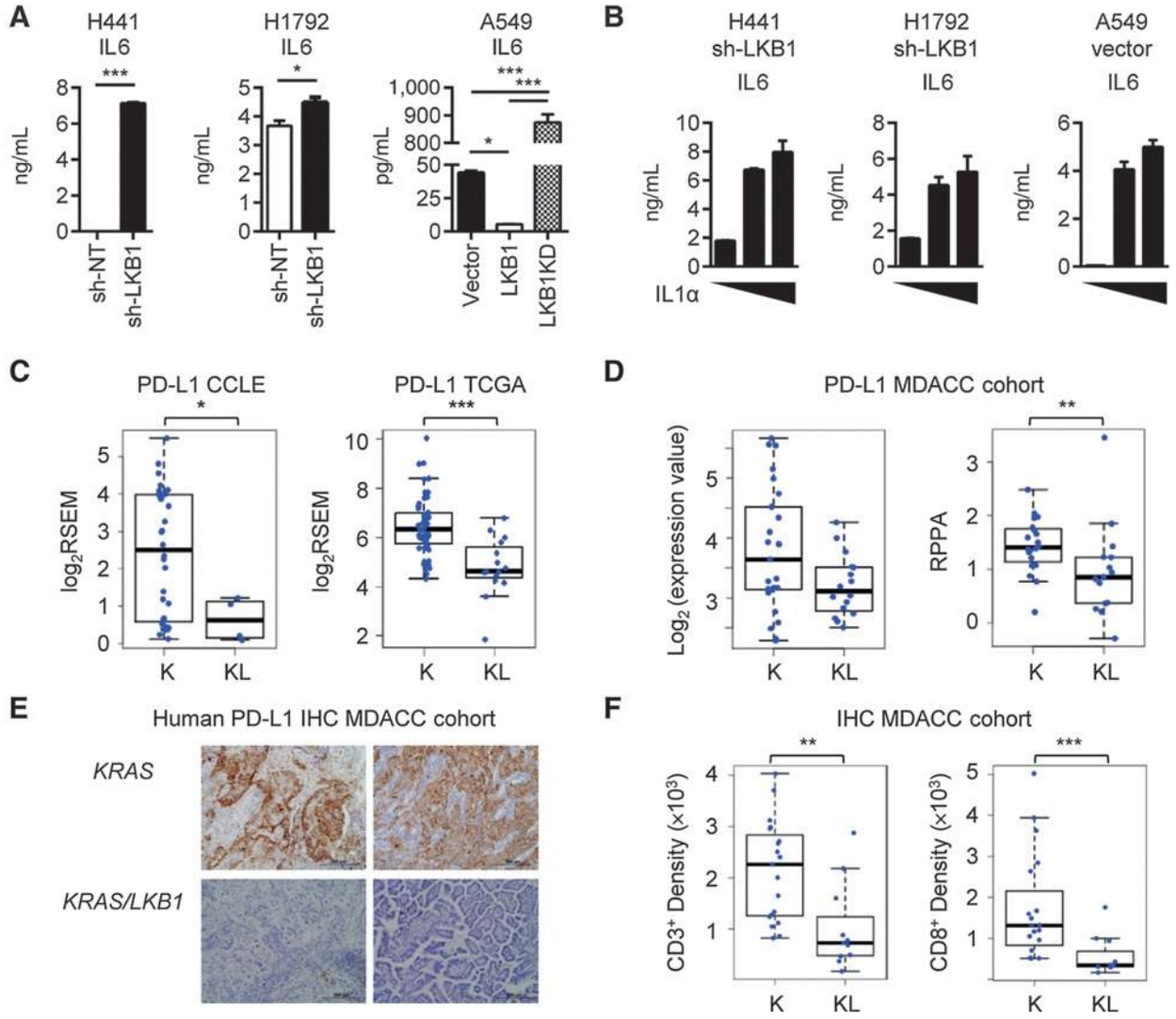

Figure 3.
LKB1 inactivation in human *KRAS*-mutated cell lines showed similar phenotype with mouse *Kras/Lkb1* tumor. A, analysis of IL6 in the culture supernatants after 48-hour incubation of *KRAS*-mutated *LKB1* wild-type H441 or H1792 cells stably transfected with sh-NT or sh-LKB1 and *KRAS*, *LKB1*-mutant A549 cells reconstituted with empty vector (Vector), wild-type LKB1, or kinase dead LKB1 (LKB1KD). *, $P < 0.05$; ***, $P < 0.001$. Data indicate three replicate wells and are representative of three independent experiments. B, IL6 levels in culture supernatants measured 24 hours after IL1α stimulation (0, 5, and 20 ng/mL) of three *LKB1*-deficient cell lines. Data indicate three replicate wells and are representative of three independent experiments. C, *PDL1* expression in *KRAS* (K) or *KRAS* and *LKB1* mutated (KL) cell lines from CCLE database (*, $P = 0.04$) and *PDL1* expression in *Kras* (K) or *Kras/Lkb1* (KL) lung adenocarcinoma samples from TCGA database (***, $P = 0.00004$). D, *PD-L1* mRNA levels determined by microarray ($P = 0.1$) and protein levels (**, $P = 0.009$) determined by RPPA from the MDACC dataset. E, representative IHC for PD-L1 on the *KRAS*-mutated *LKB1* wt or mutant patient tumors from the MDACC cohort. F, CD3 (**, $P = 0.002$)- and CD8 (***, $P = 0.0003$)-positive cell densities by IHC on the MDACC patient cohorts.

Analysis of lung cancer cell lines from The Cancer Cell Line Encyclopedia (CCLE; ref. 27) confirmed that PD-L1 expression is significantly lower in cell lines with *LKB1* mutation (32 *LKB1* WT and 4 *LKB1*-mutant cell lines; Fig. 3C), although the small number of *LKB1*-mutant lines precluded any significant associations among the immune-related genes displayed in Fig. 1C and Supplementary Fig. S2A and *LKB1* status when corrected for multiple hypotheses. In addition, analysis of *KRAS*-mutated lung adenocarcinomas from The Cancer Genome Atlas (TCGA-52 *LKB1* WT, 15 *LKB1* mutant; ref. 2) showed that PD-L1 expression was significantly reduced in *LKB1*-mutated NSCLCs (Fig. 3C). In a multivariate analysis of the TCGA dataset with respect to *LKB1* status and clinical factors, PD-L1 and *LKB1* status were also significantly associated ($P = 0.005$). To validate these findings in an independent dataset, PD-L1 mRNA was assessed in the MD Anderson PROSPECT (Profiling of Resistance Patterns and Oncogenic Signaling Pathways in Evaluation of Cancers of the Thorax and Therapeutic Target Identification) cohort (MDACC-108 *LKB1* WT, 44 *LKB1*-MUTANT cases). We again observed an association among PD-L1 expression and *LKB1* status. We also validated and quantitated the expression of PD-L1 at the protein level by reverse-phase protein arrays (RPPA) in 106 cases from the MDACC cohort

Downloaded from http://aacrjournals.org/cancerres/article-pdf/76/5/999/2746958/999.pdf by guest on 24 August 2022

and detected significantly lower levels of PD-L1 in *LKB1*-mutant tumors (Fig. 3D). As the current clinical standard detection method for the PD-L1 expression is IHC, we confirmed the difference in PD-L1 expression by IHC (Fig. 3E).

Next, to evaluate the functional effect of *LKB1*-loss in the tumor microenvironment in patient tumors, we analyzed the T-cell infiltrate in the tumors by IHC. In 19 *LKB1* WT and 11 *LKB1*-mutant tumors, total T-cell ($CD3^+$) and CD8 T-cell counts and densities were significantly lower in *LKB1*-inactivated tumors as compared with *LKB1*-intact tumors (Fig. 3F), In sum, observations in patient cell lines and tumor samples are consistent with our findings in *Kras/Lkb1* mice, suggesting that *LKB1* mutation negatively regulates PD-L1 expression and reduces CD8 T-cell infiltration.

Neutralizing IL6 leads to a therapeutic benefit in *Kras/Lkb1* mice

Supporting the notion that PD-L1 expression in tumor cells is critical in the response to PD-1 blockade, treatment of the *Kras/Lkb1* mouse model with a PD-1 blocking antibody did not show a significant treatment response (Fig. 4A). Given our observation of elevated IL1α and IL6 in BALFs (Fig. 1E and G) and aberrant activation of pSTAT3 in tumor nodules (Fig. 1F) from *Kras/Lkb1* mice as compared with *Kras* mice, we hypothesized that targeting aberrant cytokine production could be a rational therapeutic strategy in *Kras/Lkb1*–mutant tumors. To evaluate the *in vivo* efficacy of IL6 blockade, we treated *Kras/Lkb1* mice with a neutralizing IL6 antibody (MP5-20F3). The therapeutic anti-IL6 antibody significantly inhibited tumor progression as compared with anti PD-1 antibody (Fig. 4A). In addition, IL6 antibody–treated mice showed significantly improved survival as compared with control mice (Fig. 4B). However, treatment of *Kras/Lkb1* tumors with other checkpoint-blocking antibodies against CTLA-4 or a combination of PD-1 and TIM-3 also did not demonstrate any efficacy (data not shown). Taken together, these findings suggest that *Lkb1*-loss results in a T-cell–suppressed environment as a consequence of autocrine and neutrophil-induced cytokine

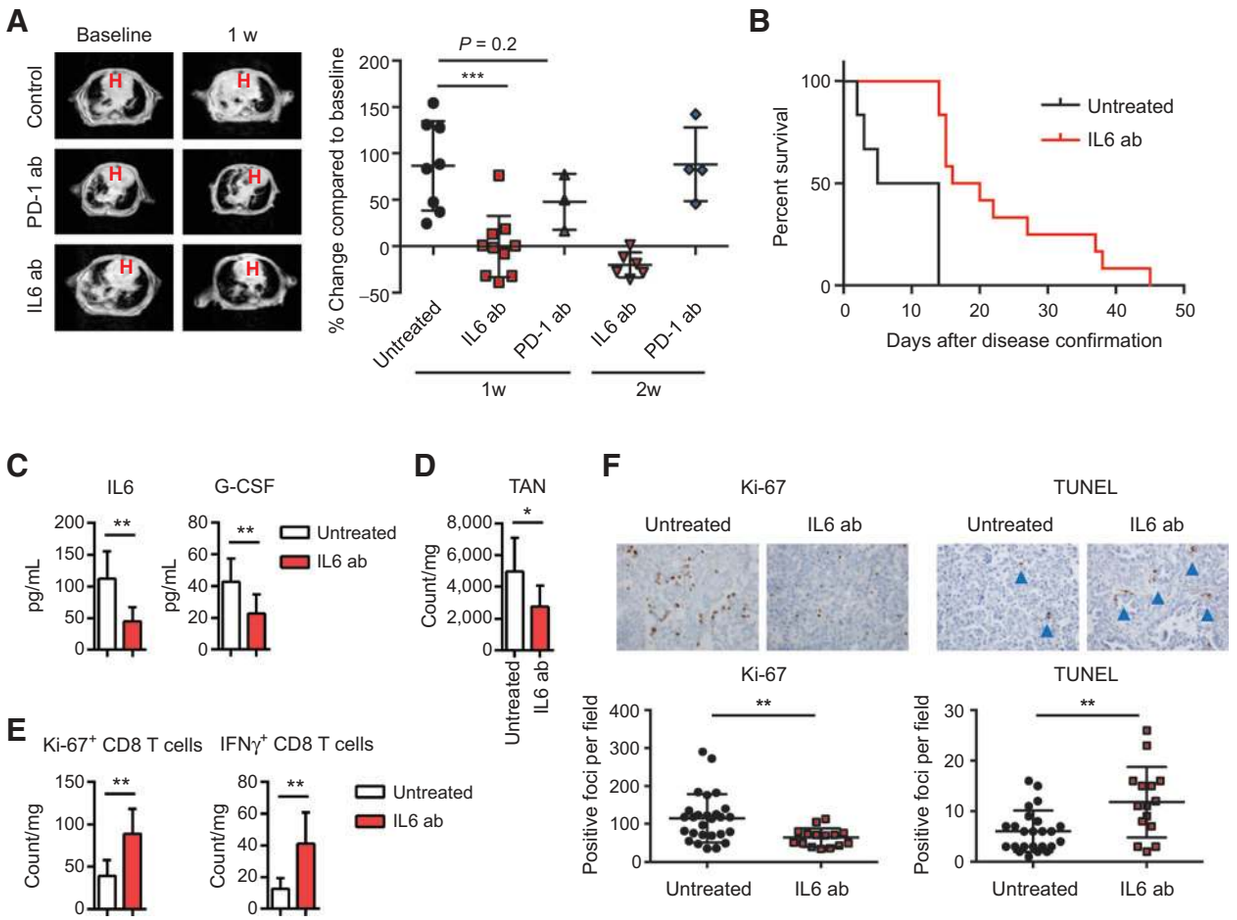

Figure 4.
IL6-neutralizing treatment showed clinical efficacy in *Kras/Lkb1* mouse model. A, representative images of MRI and quantification of MRI from KL mice treated with PD-1 or IL6-blocking antibodies or controls. B, survival of untreated mice versus mice treated with IL6-blocking antibody (***, $P = 0.0002$, $n = 6$ vs. 12, respectively). C and D, IL6 and G-CSF levels in BALFs (C) and TAN counts (D) for untreated KL mice ($n = 7$) or KL mice treated with IL6-neutralizing antibody ($n = 8$), with comparable tumor burden. *, $P < 0.05$; **, $P < 0.01$. E, Ki-67 and IFNγ-positive CD8 T-cell counts in untreated KL mice ($n = 7$) or KL mice treated with IL6-neutralizing antibody ($n = 8$), with comparable tumor burden. F, representative Ki-67 and TUNEL IHC and quantification per the microscopic field on the KL mice untreated or treated with IL6-neutralizing antibody. Each data point represents a different microscopic field. For Ki-67, $n = 9$ and 5 and for TUNEL, $n = 8$ and 5 for untreated and IL6 antibody (ab)-treated mice, respectively. **, $P = 0.0049$ for Ki-67; **, $P = 0.0024$ for TUNEL.

Downloaded from http://aacrjournals.org/cancerres/article-pdf/76/5/999/2746958/999.pdf by guest on 24 August 2022

production and not engagement of the PD-L1:PD-1 immune checkpoint.

To further investigate the effect of IL6–neutralizing antibody on the immune profile of *Kras/Lkb1* tumors, we treated the mice for 2 weeks and then performed immune and histologic analyses (Supplementary Fig. S6A). There was a significant reduction in detectable IL6 as expected as well as G-CSF in BALFs from the treated mice (Fig. 4C). In keeping with the neutrophil-attracting cytokines and chemokines observed in BALFs, there was a significant reduction in the counts of total TAN with IL6 neutralization (Fig. 4D), resulting in functional recovery of T cells (Fig. 4E). Treated tumors also exhibited elevation of CD4 T cells, CD8 T cells, and TAM to levels that are comparable with the *Lkb1* wild-type tumors (Supplementary Fig. S6B). In addition to the immune-related effects, IL6 antibody–treated tumor cells exhibited significantly less proliferation and increased apoptosis (Fig. 4F). Although therapeutic IL6 blockade improved T-cell function, concurrent therapy combining anti-IL6 and PD-1 treatment did not demonstrate additional benefit as compared with IL6 blockade alone in terms of survival (Supplementary Fig. S6C). This suggests a need to further define contexts in which cytokine suppression and immune checkpoint blockade might be utilized together to enhance therapeutic benefit as compared with either treatment alone.

Discussion

Oncogenes and tumor suppressors promote self-sufficient signaling for autonomous proliferation of tumor cells. Recent work has shown that oncogenic mutations alter the tumor microenvironment, cause immune suppression, and can impact the response to immune-modulating treatment strategies (10). Somatic mutations also produce neoantigens, which are recognized by the immune system and mediate sensitivity of the tumors to immunotherapies (28–30). Here, we have shown that inactivation of the tumor suppressor gene *STK11/LKB1* causes dramatic changes in the tumor microenvironment in addition to the previously reported effects on cell cycle, metabolism, differentiation, polarity, and other cellular pathways (16, 31).

We have shown that *LKB1* inactivation promoted the production of proinflammatory cytokines CXCL7, G-CSF, and IL6 in both mouse tumors and cell lines, which contributes to neutrophil accumulation. Elevation of the proinflammatory cytokine IL1α was confirmed *in vivo* but not robustly in cell culture supernatants from *Lkb1*-deficient cells. Previous studies have shown that IL1α is released only under specific conditions including necrotic cell death and inflammasome activation (32, 33), suggesting that the release of IL1α could be caused by necrotic cell death in *Kras/Lkb1* tumor microenvironment and that this facilitates the activation of IL6–STAT3 signaling pathway in *Kras/Lkb1* tumors together with IL6, producing neutrophil accumulation.

The tumor microenvironment in *Kras/Lkb1* tumors displayed characteristics of T-cell suppression with fewer lymphocytes, higher levels of checkpoint receptor expression in those, and an increase in TANs with suppressive properties compared with *Kras* tumors. TANs expressing high levels of *Il10*, *Arginase1*, and *Mfge8* that have been implicated in T-cell suppression and Treg induction (15, 22, 34). Depleting TAN using an anti Ly-6G/Gr-1 antibody improved T-cell function. Although the role of TAN in suppressing T-cell function is controversial (35), TAN appear to act in an immunosuppressive fashion in this context, suggesting that therapies suppressing TAN should be further explored as immunomodulatory therapies.

Moreover, we found that *Lkb1* inactivation caused a decrease in PD-L1 levels on tumor cells from *Kras/Lkb1* tumors and in cultured cells from mice and patients. Conforming to the previous observations proposing an association of tumor cell PD-L1 expression, the magnitude of T-cell accumulation in the tumors and response to PD-1 blockade (7, 8, 36), treatment with a PD-1–blocking antibody did not show efficacy in the treatment of the *Kras/Lkb1* mouse model. A recent study (30) as well as our own institutional experience suggest that while *KRAS*-mutated patients respond favorably to PD-1 blockade (PFS of 15 months on pembrolizumab) this is not seen in patients with *LKB1* mutations although large cohorts will be needed to define genotype–response associations in detail. In addition, contributing to low PD-1:PD-L1 levels in *Kras/Lkb1* tumors is the greater proportion of TAN that express low levels of PD-L1 as compared with TAM. The coordinated role of PD-L1 expression in the tumor cells and the cells constituting the immune microenvironment in this model requires further study to define improved immunotherapeutic strategies.

Treatment of *Kras/Lkb1* tumors with an IL6–blocking antibody decreased tumor cell proliferation and increased T-cell function, resulting in a therapeutic effect in *Kras/Lkb1* mouse model while immune checkpoint blockade was not efficacious. These data suggest that mouse models can be used to model the tumor microenvironment and predict response to novel immune-modulating treatment strategies based on rational predictions from studies of the tumor microenvironment. Future studies will examine whether cytokines other than IL6 also contribute to STAT3 activation (37), and whether combined cytokine blockade (e.g., with IL1 neutralization) will lead to more durable therapeutic effects. Although we found that neutralizing IL6 antibodies improved T-cell number and function in Lkb1-deficient tumors, the combination of anti PD-1 plus anti IL6 antibodies did not improve outcome when given concurrently. There may be technical limitations to this considering both of the antibodies are Rat IgG isotype and combination treatment can lead to antibody neutralization. Furthermore, dosing schedules of cytokine suppression and combinations with other therapeutic agents such as immune checkpoint blockade will need to be studied.

In summary, we have presented a novel set of findings that suggest that not only oncogene driver mutations but also tumor suppressor gene mutations can modify the immune microenvironment in lung cancer. In this example, focusing on *Lkb1* loss, we observed a marked increase in inflammatory cytokines that recruited neutrophils and inhibited the function of T cells. We also showed that PD-1 checkpoint blockade was ineffective in *Lkb1*-mutant cancers, whereas targeting IL6 displayed a significant albeit short-lived treatment response in the *Kras/Lkb1* model. These findings suggest that IL6-dependent signaling activation can be a therapeutic target in *Lkb1*-deficient *Kras*-driven lung tumors and potentially other tumors with high levels of IL6, and also suggest targeting aberrant inflammation by inhibiting cytokine signaling may represent a promising immunotherapeutic strategy in selected patients.

Disclosure of Potential Conflicts of Interest

M. Hellmann reports receiving a commercial research grant from Bristol-Myers Squibb and is a consultant/advisory board member for Bristol-Myers

Downloaded from http://aacrjournals.org/cancerres/article-pdf/76/5/999/2746958/999.pdf by guest on 24 August 2022

Squibb, Genentech, Third Rock Ventures, and Inovio Pharmaceuticals. J.V. Heymach reports receiving other commercial research support from AstraZeneca, GlaxoSmithKline, Bayer and is a consultant/advisory board member for Genentech, AstraZeneca, Novartis, GlaxoSmithKline, Lilly, Boerhinger Ingelheim, Synta, and Exelixis. F.S. Hodi is a consultant in Merck and reports receiving a commercial research grant from Bristol Myers Squibb and Merck (to institution). G.J. Freeman has ownership interest (including patents) in Merck, Bristol Myers Squibb, Roche (immediate family member), EMD Serono, Amplimmune, Boehringer Ingelheim, Novartis (immediate family member) and is a consultant/advisory board member for Novartis (immediate family member), Roche, Bristol Myers Squibb, Eli Lilly, and Surface Oncology (immediate family member). D.A. Barbie is a consultant/advisory board member for N-of-One. G. Dranoff is a global head, exploratory immune-oncology in Novartis. No potential conflicts of interest were disclosed by the other authors.

Authors' Contributions

Conception and design: S. Koyama, E.A. Akbay, G.S. Herter-Sprie, P.E. Fecci, J.V. Heymach, G. Dranoff, P.S. Hammerman, K.-K. Wong
Development of methodology: S. Koyama, E.A. Akbay, A.R. Aref, F. Skoulidis, G.J. Freeman
Acquisition of data (provided animals, acquired and managed patients, provided facilities, etc.): S. Koyama, E.A. Akbay, F. Skoulidis, G.S. Herter-Sprie, K.A. Buczkowski, Y. Liu, M.M. Awad, E.R. Parra Cuentas, I.I. Wistuba, M. Soucheray, H. Asahina, S. Kitajima, A. Altabef, J.D. Cavanaugh, K. Rhee, P.E. Fecci, T. Shimamura, M. Hellmann, J.V. Heymach, F.S. Hodi, D.A. Barbie, K.-K. Wong
Analysis and interpretation of data (e.g., statistical analysis, biostatistics, computational analysis): S. Koyama, E.A. Akbay, Y.Y. Li, F. Skoulidis, G.S. Herter-Sprie, K.A. Buczkowski, Y. Liu, M.M. Awad, W.L. Denning, L. Diao, J. Wang, E.R. Parra Cuentas, I.I. Wistuba, S. Kitajima, F.S. Hodi, D.A. Barbie, G. Dranoff, P.S. Hammerman
Writing, review, and/or revision of the manuscript: S. Koyama, E.A. Akbay, Y.Y. Li, F. Skoulidis, G.S. Herter-Sprie, K.A. Buczkowski, H. Zhang, M. Hellmann, J.V. Heymach, F.S. Hodi, G.J. Freeman, G. Dranoff, P.S. Hammerman, K.-K. Wong
Administrative, technical, or material support (i.e., reporting or organizing data, constructing databases): G.S. Herter-Sprie, Y. Liu, K. Rhee, P. Gao, H. Zhang, J.V. Heymach, G.J. Freeman, P.S. Hammerman
Study supervision: D.A. Barbie, G. Dranoff, P.S. Hammerman, K.-K. Wong
Other (pathology involving in the data analysis): E.R. Parra Cuentas
Other (Western blot analysis): T. Thai
Other (construction of cell line models): T. Shimamura

Acknowledgments

The authors thank Suzan Lazo-Kallanian, John Daley, Kristen Cowens, and Steven Paul for help with flow cytometry anlaysis, Christine Lam for tissue processing, Mei Zhang for IHC, Xiaoen Wang for helping with mouse studies, and the Dana Farber Center for Cancer Genome Discovery for RNA sequencing.

Grant Support

P.S. Hammerman is supported by a Clinical Investigator Award from the Damon Runyon Cancer Research Foundation, a Developmental Project Grant from NCI P50 CA090578 and the Starr Consortium for Cancer Research. K.-K. Wong is supported by NIH/NCI P01 CA120964, 5R01CA163896-04, 1R01CA195740-01, 5R01CA140594-07, 5R01CA122794-10, and 5R01CA166480-04 grants and support from Gross-Loh Family Fund for Lung Cancer Research and Susan Spooner Family Lung Cancer Research Fund at Dana-Farber Cancer Institute. P.S. Hammerman, K.K. Wong, J.V. Heymach, and M.D. Hellman are supported by a Stand Up To Cancer - American Cancer Society Lung Cancer Dream Team Translational Research Grant (Grant Number: SU2C-AACR-DT17-15). Stand Up To Cancer is a program of the Entertainment Industry Foundation. Research grants are administered by the American Association for Cancer Research, the scientific partner of SU2C. S. Koyama is supported by Margaret A. Cunningham Immune Mechanisms in Cancer Research Fellowship Award and The Kanae Foundation for the Promotion of Medical Science Fellowship Award. G.S. Herter-Sprie was supported by the Deutsche Forschungsgemeinschaft (HE 6897/1-1) and the Claudia Adams Barr Program for Innovative Cancer Research. T. Shimamura is supported by Uniting Against Lung Cancer Legacy Program and American Cancer Society Research Scholar Award. G.J. Freeman is supported by NIH R01AI08995.

Received May 29, 2015; revised November 24, 2015; accepted December 6, 2015; published OnlineFirst February 1, 2016.

References

1. Cardarella S, Johnson BE. The impact of genomic changes on treatment of lung cancer. Am J Respir Crit Care Med 2013;188:770–5.
2. The Cancer Genome Atlas Network. Comprehensive molecular profiling of lung adenocarcinoma. Nature 2014;511:543–50.
3. Ji H, Ramsey MR, Hayes DN, Fan C, McNamara K, Kozlowski P, et al. LKB1 modulates lung cancer differentiation and metastasis. Nature 2007;448:807–10.
4. Chen Z, Cheng K, Walton Z, Wang Y, Ebi H, Shimamura T, et al. A murine lung cancer co-clinical trial identifies genetic modifiers of therapeutic response. Nature 2012;483:613–7.
5. Zhao N, Wilkerson MD, Shah U, Yin X, Wang A, Hayward MC, et al. Alterations of LKB1 and KRAS and risk of brain metastasis: comprehensive characterization by mutation analysis, copy number, and gene expression in non-small-cell lung carcinoma. Lung Cancer 2014;86:255–61.
6. Calles A, Sholl LM, Rodig SJ, Pelton AK, Hornick JL, Butaney M, et al. Immunohistochemical loss of LKB1 is a biomarker for more aggressive biology in KRAS mutant lung adenocarcinoma. Clin Cancer Res 2015;21:2851–60.
7. Taube JM, Klein A, Brahmer JR, Xu H, Pan X, Kim JH, et al. Association of PD-1, PD-1 ligands, and other features of the tumor immune microenvironment with response to anti-PD-1 therapy. Clin Cancer Res 2014;20:5064–74.
8. Tumeh PC, Harview CL, Yearley JH, Shintaku IP, Taylor EJ, Robert L, et al. PD-1 blockade induces responses by inhibiting adaptive immune resistance. Nature 2014;515:568–71.
9. Herbst RS, Soria JC, Kowanetz M, Fine GD, Hamid O, Gordon MS, et al. Predictive correlates of response to the anti-PD-L1 antibody MPDL3280A in cancer patients. Nature 2014;515:563–7.
10. Akbay EA, Koyama S, Carretero J, Altabef A, Tchaicha JH, Christensen CL, et al. Activation of the PD-1 pathway contributes to immune escape in EGFR-driven lung tumors. Cancer Discov 2013;3:1355–63.
11. Ochoa CE, Mirabolfathinejad SG, Ruiz VA, Evans SE, Gagea M, Evans CM, et al. Interleukin 6, but not T helper 2 cytokines, promotes lung carcinogenesis. Cancer Prev Res 2011;4:51–64.
12. Ancrile B, Lim KH, Counter CM. Oncogenic Ras-induced secretion of IL6 is required for tumorigenesis. Genes Dev 2007;21:1714–9.
13. Barbie DA, Tamayo P, Boehm JS, Kim SY, Moody SE, Dunn IF, et al. Systematic RNA interference reveals that oncogenic KRAS-driven cancers require TBK1. Nature 2009;462:108–12.
14. Meylan E, Dooley AL, Feldser DM, Shen L, Turk E, Ouyang C, et al. Requirement for NF-kappaB signalling in a mouse model of lung adenocarcinoma. Nature 2009;462:104–7.
15. Motz GT, Coukos G. Deciphering and reversing tumor immune suppression. Immunity 2013;39:61–73.
16. Liu Y, Marks K, Cowley GS, Carretero J, Liu Q, Nieland TJ, et al. Metabolic and functional genomic studies identify deoxythymidylate kinase as a target in LKB1-mutant lung cancer. Cancer Discov 2013;3:870–9.
17. Shimamura T, Chen Z, Soucheray M, Carretero J, Kikuchi E, Tchaicha JH, et al. Efficacy of BET bromodomain inhibition in Kras-mutant non-small cell lung cancer. Clin Cancer Res 2013;19:6183–92.
18. Zhu Z, Aref AR, Cohoon TJ, Barbie TU, Imamura Y, Yang S, et al. Inhibition of KRAS-driven tumorigenicity by interruption of an autocrine cytokine circuit. Cancer Discov 2014;4:452–65.
19. Tchaicha JH, Akbay EA, Altabef A, Mikse OR, Kikuchi E, Rhee K, et al. Kinase domain activation of FGFR2 yields high-grade lung adenocarcinoma sensitive to a Pan-FGFR inhibitor in a mouse model of NSCLC. Cancer Res 2014;74:4676–84.

Downloaded from http://aacrjournals.org/cancerres/article-pdf/76/5/999/2746958/999.pdf by guest on 24 August 2022

20. Franciszkiewicz K, Boutet M, Gauthier L, Vergnon I, Peeters K, Duc O, et al. Synaptic release of CCL5 storage vesicles triggers CXCR4 surface expression promoting CTL migration in response to CXCL12. J Immunol 2014;193: 4952–61.
21. Luther SA, Bidgol A, Hargreaves DC, Schmidt A, Xu Y, Paniyadi J, et al. Differing activities of homeostatic chemokines CCL19, CCL21, and CXCL12 in lymphocyte and dendritic cell recruitment and lymphoid neogenesis. J Immunol 2002;169:424–33.
22. Najjar YG, Finke JH. Clinical perspectives on targeting of myeloid derived suppressor cells in the treatment of cancer. Front Oncol 2013;3:49.
23. Walker F, Zhang HH, Matthews V, Weinstock J, Nice EC, Ernst M, et al. IL6/sIL6R complex contributes to emergency granulopoietic responses in G-CSF- and GM-CSF-deficient mice. Blood 2008;111:3978–85.
24. Suzuki E, Mellins ED, Gershwin ME, Nestle FO, Adamopoulos IE. The IL-23/IL-17 axis in psoriatic arthritis. Autoimmun Rev 2014;13:496–502.
25. Leslie K, Gao SP, Berishaj M, Podsypanina K, Ho H, Ivashkiv L, et al. Differential interleukin-6/Stat3 signaling as a function of cellular context mediates Ras-induced transformation. Breast Cancer Res 2010;12:R80.
26. Rodig N, Ryan T, Allen JA, Pang H, Grabie N, Chernova T, et al. Endothelial expression of PD-L1 and PD-L2 down-regulates CD8+ T cell activation and cytolysis. Eur J Immunol 2003;33:3117–26.
27. Barretina J, Caponigro G, Stransky N, Venkatesan K, Margolin AA, Kim S, et al. The Cancer Cell Line Encyclopedia enables predictive modelling of anticancer drug sensitivity. Nature 2012;483:603–7.
28. Gubin MM, Zhang X, Schuster H, Caron E, Ward JP, Noguchi T, et al. Checkpoint blockade cancer immunotherapy targets tumour-specific mutant antigens. Nature 2014;515:577–81.
29. Yadav M, Jhunjhunwala S, Phung QT, Lupardus P, Tanguay J, Bumbaca S, et al. Predicting immunogenic tumour mutations by combining mass spectrometry and exome sequencing. Nature 2014;515:572–6.
30. Rizvi NA, Hellmann MD, Snyder A, Kvistborg P, Makarov V, Havel JJ, et al. Cancer immunology. Mutational landscape determines sensitivity to PD-1 blockade in non-small cell lung cancer. Science 2015;348:124–8.
31. Skoulidis F, Byers LA, Diao L, Papadimitrakopoulou VA, Tong P, Izzo J, et al. Co-occurring genomic alterations define major subsets of KRAS-mutant lung adenocarcinoma with distinct biology, immune profiles, and therapeutic vulnerabilities. Cancer Discov 2015;5:860–77.
32. Chen GY, Nunez G. Sterile inflammation: sensing and reacting to damage. Nat Rev Immunol 2010;10:826–37.
33. Voronov E, Dotan S, Krelin Y, Song X, Elkabets M, Carmi Y, et al. Unique versus redundant functions of IL-1alpha and IL-1beta in the tumor microenvironment. Front Immunol 2013;4:177.
34. Jinushi M, Hodi FS, Dranoff G. Enhancing the clinical activity of granulocyte-macrophage colony-stimulating factor-secreting tumor cell vaccines. Immunol Rev 2008;222:287–98.
35. Eruslanov EB, Bhojnagarwala PS, Quatromoni JG, Stephen TL, Ranganathan A, Deshpande C, et al. Tumor-associated neutrophils stimulate T cell responses in early-stage human lung cancer. J Clin Invest 2014;124: 5466–80.
36. Garon EB, Rizvi NA, Hui R, Leighl N, Balmanoukian AS, Eder JP, et al. Pembrolizumab for the treatment of non-small-cell lung cancer. N Engl J Med 2015;372:2018–28.
37. Yu H, Pardoll D, Jove R. STATs in cancer inflammation and immunity: a leading role for STAT3. Nat Rev Cancer 2009;9:798–809.

Downloaded from http://aacrjournals.org/cancerres/article-pdf/76/5/999/2746958/999.pdf by guest on 24 August 2022